

Surface Crystallography of YSi_{2-x} Films Epitaxially Grown on Si(111): An X-Ray Photoelectron Diffraction Study

R. Baptist,⁽¹⁾ S. Ferrer,⁽²⁾ G. Grenet,⁽³⁾ and H. C. Poon⁽³⁾

⁽¹⁾*Département Optronique, Division Laboratoire d'Electronique et de Technologie de l'Informatique, Centre d'Etudes Nucléaires de Grenoble 85 X, F38041, Grenoble CEDEX, France*

⁽²⁾*European Synchrotron Radiation Facility, Boîte Postale No. 220, F38043, Grenoble CEDEX, France*

⁽³⁾*Institut de Physique Nucléaire et Université Claude Bernard, Lyon I, 43, Bd du 11 novembre 1918, F69622, Villeurbanne CEDEX, France*

(Received 16 May 1989)

The surface crystallography of epitaxially grown YSi_{2-x} ($x=0.3$ and $x=0$) films on Si(111) has been investigated using x-ray photoelectron diffraction. For the $\text{YSi}_{1.7}$ films, vacancies form an ordered $\sqrt{3} \times \sqrt{3} R30^\circ$ superlattice within each Si plane. These vacancies are filled for YSi_2 . The analysis reveals that their surfaces are Si terminated with a displacement upward (0.8 Å) of one Si atom out of two so that they exhibit the same geometry as a (1×1) Si(111) surface.

PACS numbers: 79.60.Eq, 73.60.Gx, 81.15.Gh

One of the milestones in atomic engineering of new materials of technological and scientific interest is to achieve the fabrication of heteroepitaxial systems with a high degree of crystallinity and structural perfection, containing interfaces as close to ideal as possible, i.e., chemically sharp, topographically flat, and without structural defects. In this context, much work¹⁻³ has been made to grow, characterize, and study the transition-metal silicides grown epitaxially on Si(111) such as CoSi_2 and NiSi_2 which have a rather good lattice match relative to the Si(111) surface lattice (1.3% and 0.4%, respectively).

The aim of this Letter is to present new structural information of YSi_{2-x} epitaxially grown on Si(111) which presents an ideal 0.0% lattice mismatch relative to the Si(111) surface lattice. A consequence of this 0.0% value is a possibility to grow large perfect surfaces of Y silicide on Si(111).⁴⁻⁷ Moreover, the abruptness of the silicide/vacuum interface makes it feasible to overgrow the YSi_{2-x} with epitaxial Si.⁸ As for its applications in technology, the potential advantage⁹ of the thermally oxidized yttrium film Y_2O_3 on silicon should also be mentioned: The combination of the Y-silicide electrical properties (very-low-Schottky-barrier height $\phi \sim 0.3-0.4$ eV on *n*-type Si) and of the Y-oxide dielectric properties (high dielectric constant $\epsilon \sim 14-17$) offers new perspectives in device technology.

The $\text{YSi}_{1.7}$ crystallographic structure consists of Y planes alternating with Si planes parallel to the Si(111) substrate planes. Within each plane, the atoms are arranged in a planar mesh with sixfold symmetry where one Si atom out of six is missing (stoichiometry 1:1.7 instead of 1:2) leading to the formation of an ordered superlattice of vacancies. The distances Y-Y, Y-Si, and Si-Si (3.84, 3.03, and 2.2 Å, respectively) are very different from typical values found for other transition-metal silicides (metal-metal ~ 3.2 Å, metal-Si ~ 2.6 Å,

and Si-Si ~ 2.6 Å) due to the "graphitic"-type bonding of the Si atoms.¹⁰

In view of the above-mentioned important technological applications, we have focused our attention on the surface structural characteristics of YSi_{2-x} , one of the most interesting epitaxial silicides known to date. In this respect, we have used x-ray photoelectron diffraction (XPD) which appears as direct real-space scans.¹¹⁻¹⁷

The experimental XPD apparatus consists of a VG-ESCALAB (with a standard Al $K\alpha$ radiation source $h\nu = 1486.6$ eV) which is connected to a sample preparation chamber with Y and Si evaporators, sample heating, and a low-energy electron diffractometer (LEED). A high-precision manipulator allows angular rotations of *in situ* grown samples. The acceptance angle of the spectrometer controlled by a removable diaphragm is 2° . The basic details concerning the XPD data recording and normalization may be found in Ref. 18.

The silicide films were prepared as follows. First, a Y film (~ 15 nm) was deposited on a clean Si(111) surface exhibiting a good (7×7) LEED pattern. After deposition, the reaction Si+Y was sustained at $\sim 450^\circ\text{C}$ until the characteristic LEED pattern of $\text{YSi}_{1.7}$ was obtained. This 1:1.7 stoichiometry (1.65-1.7 for all cases studied), as determined by angle-integrated x-ray photoemission, is due to an ordered superlattice in the bulk which produces a $\sqrt{3} \times \sqrt{3} R30^\circ$ superstructure at the surface.^{5,8} Such samples will be referred to as sample *A* in the following. Samples *B* are samples *A* on which two additional treatments were performed: a new deposit of Si (~ 10 nm), followed by an annealing at $900-1000^\circ\text{C}$ until grazing angle x-ray photoemission spectroscopy revealed a surface concentration ratio of Si to Y close to 1:2 and a (1×1) LEED pattern.

The YSi_{2-x} has a AlB_2 bulk structure.⁴ Figure 1 shows the projection of the stoichiometric YSi_2 structure on some low-index planes. The $\phi = 0^\circ$ planes (defined by

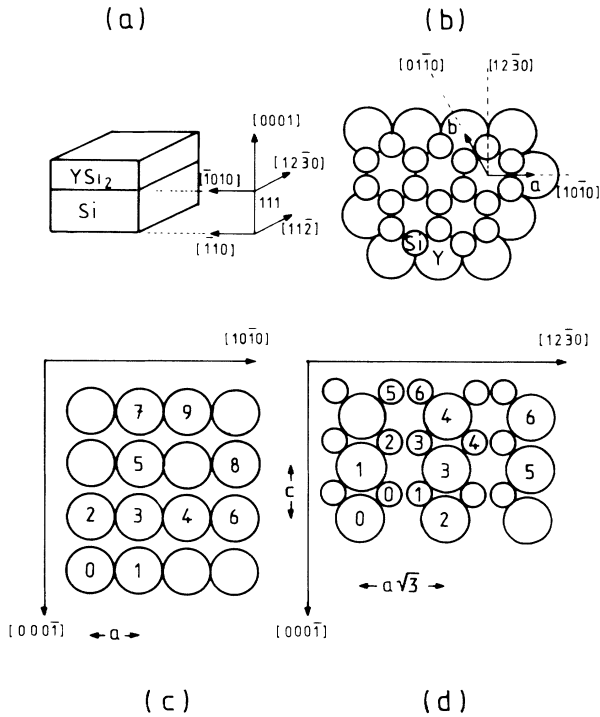


FIG. 1. Crystallographic structure of the YSi_2 silicide: (a) Lattice axis definition for epitaxially grown YSi_2 on $Si(111)$. (b) Si and Y planes perpendicular to the $[111]$ direction. (c) Si or Y planes referred as $\phi=0^\circ$ planes; numbering refers to this plane. (d) Si and Y planes referred as $\phi=30^\circ$ planes; numbering refers to this plane and is independent of (c).

the directions $[10\bar{1}0]$ and $[000\bar{1}]$ contain either Y or Si atoms but the $\phi=30^\circ$ planes (defined by the directions $[12\bar{3}0]$ and $[000\bar{1}]$) contain both Y and Si atoms. The values of the lattice constants $a=3.84 \text{ \AA}$ and $c=4.14 \text{ \AA}$ have been checked using high-energy electron diffraction. The main internuclear axis angles are listed in Table I for Y and Si emitters.

A previous study by electron microscopy⁸ has revealed an ordered bulk superstructure:^{5,7} In a given $Si[0001]$ plane, one atom from six is missing (Fig. 2). The plane just below the Si plane has the same structure but is rotated by 120° . The next plane is rotated by -120° and thus is identical to the first one. These vacancies give the $\sqrt{3} \times \sqrt{3} R30^\circ$ mesh in a Si plane observable by LEED. In view of the discussion below, we have also indicated (crosses) in Fig. 2 the positions of vertically displaced (0.8 \AA) Si atoms (Si^{up}) in accordance with a pure Si lattice (last columns in Table I).

In Fig. 3, experimental polar plots of Y $3d$ and Si $2p$ core levels are shown for $\phi=0^\circ$ and 30° for both samples A and B. The Si surface enrichment of the sample B as compared with the sample A produces an increase of intensity at grazing angles in Figs. 3(c) and 3(d). A close correspondence is immediately obvious between the XPD peaks and the angles listed in Table I. Since the $\phi=0^\circ$

plane geometries are the same for Y and Si atoms, enhancements appear at the same polar angles in Figs. 3(a) and 3(c). However, the XPD anisotropy is weaker for Si $2p$ emission than for Y $3d$ emission because of the smaller scattering efficiency of Si ($Z=14$) than of Y ($Z=39$). In Figs. 3(a) and 3(c), the particularly well defined $\theta=43^\circ$ peak corresponds to a first-neighbor direction between an emitter of the second layer and a scatterer of the top layer. Turning now to $\phi=30^\circ$, the two kinds of emitter scatterer may be identified: clearly in Fig. 3(b) for Y-Y at $\theta=58^\circ$ and 39° and Y-Si at $\theta=47^\circ$, 65° , 20° , and 36° and weakly but still present in Fig. 3(d) for Si_0 -Y at $\theta=65^\circ$ and 36° and for Si_1 -Y at $\theta=47^\circ$ and 20° . The Si-Si enhancements are too small in Fig. 3(d) to be observed due to the low Si atomic number. The weakness of the Si-Y enhancements is an indication of the presence of a Si top layer which produces an isotropic emission. Furthermore, the two different Si sites contained in $\phi=30^\circ$ planes lead to two superposed diffraction patterns and thus to an averaged XPD pattern.

The actual XPD spectra are more complicated due to the presence of secondary diffraction effects off internuclear axes¹³ and multiple-scattering effects.¹⁹ To evaluate them, we have performed multiple-scattering calculations using the quasidynamical method.²⁰ We have neglected all multiple scatterings within the same layer and all backscatterings since both are small at high kinetic energies. The calculated results for a flat YSi_2 terminated surface are compared with experiments in Fig. 3: The overall agreement is good. However, it must be noticed that for the bulk terminated surface, the 39° internuclear peak is absent in the theoretical curve of Fig. 3(b). This absence may be explained by the fact that the experimental peak does not result from Y-Y diffraction since the Y neighbors are at a distance 10.6 \AA too large for the forward focusing to be effective. More likely, the presence of a well structured double peak at 39° and 47° in Fig. 3(b) suggests a surface terminated by a Si double layer, which is generally considered for the surface of Co silicide.³ As for the discrepancy at $\theta=20^\circ$ between theory and experiment in the same curve, we have performed a single-scattering calculation which reproduced the 20° peak. The split in the multiple-scattering curve is due to the multiple scattering of electrons from the second-layer Y emitters. Therefore, it is of complex origin not directly related to the geometrical structure.

In order to verify this geometry suggested by the above calculations and described in Fig. 2, let us compare the XPD curves for sample A (with vacancies) and for sample B (where the vacancies are supposed to be replaced by Si^{up} atoms at the surface). At $\phi=0^\circ$, there is an unmodified Y plane and two kinds of Si planes (labeled 1 and 2 in Fig. 2). The first of these Si planes is unmodified while the second contains both vacancies and Si^{up} atoms. The consequence of this buckling is thus ex-

TABLE I. Internuclear axis with bulk Y and Si as emitter for azimuthal planes $\phi=0^\circ$ and 30° . Polar angles θ_A and lengths L_A correspond to unmodified Si top atoms while θ_B and L_B to upward displaced Si atoms (θ and L values are calculated for the ideal YSi_2 structure).

Emitter	Scatterer	ϕ (deg)	θ_A (deg)	L_A (Å)	θ_B (deg)	L_B (Å)
Y ₀	Y ₁	0.0	90.0	3.8		
	Y ₂		0.0	4.1		
	Y ₃		42.8	5.6		
	Y ₄		61.7	8.7		
	Y ₅		24.9	9.1		
	Y ₆		70.2	12.2		
	Y ₇		17.2	13.0		
	Y ₈		54.3	14.2		
	Y ₉		31.7	14.6		
Y ₀	Y ₁	30.0	0.0	4.1		
	Y ₂		90.0	6.7		
	Y ₃		58.1	7.8		
	Y ₄		38.8	10.6		
	Y ₅		72.7	13.9		
Y ₀	Si ₀	30.0	47.0	3.0	37.8	3.6
	Si ₁		65.0	4.9	57.3	5.3
	Si ₂		19.6	6.6	17.6	7.3
	Si ₃		35.5	7.6	32.4	8.3
Si ₀	Si ₁	0.0	90.0	3.8	78.5	3.9
	Si ₂		0.0	4.1	0.0	4.9
	Si ₃		42.8	5.6	38.0	6.2
	Si ₄		61.7	8.7	57.4	9.1
	Si ₅		24.9	9.1	23.0	9.8
	Si ₆		70.2	12.2	66.9	12.5
	Si ₇		17.2	13.0	16.1	13.7
	Si ₈		54.3	14.2	51.8	14.7
	Si ₉		31.7	14.6	30.0	15.3
Si ₀	Si ₁	30	90	2.2	70.6	2.2
	Si ₂		0.0	4.14	0.0	4.9
	Si ₃		28.2	4.7	24.3	5.4
	Si ₄		58.1	7.8	53.5	8.3
	Si ₅		15.0	8.6	13.8	9.3
Si ₀	Y ₃	30	65.0	4.9		
	Y ₄		35.5	7.7		
Si ₁	Y ₃	30	47.0	3.0		
	Y ₄		19.6	6.6		

pected to be almost absent for Y $3d$ curves and quite small for Si $2p$ curves since one out of two Si planes is unmodified and in the other one, either the emitter or the scatterer is missing. In fact, in Fig. 3(a) no real differences between samples A and B may be detected. Nevertheless, in Fig. 3(c) the polar plots are slightly changed (shaded regions) relative to one another reflecting the up displaced Si enrichment of sample B ($\theta=38^\circ$, 57° , and 23°). Looking now along the $\phi=30^\circ$ direction in Fig. 2, we find three different vertical planes (labeled 1, 2, and 3). The first plane contains, along the

$[12\bar{3}0]$ direction, the following Si top-layer sequence: {Si-vacancy} for sample A and {Si-Si^{up}} for sample B . The second plane is identical for both samples A and B and the Si top-layer sequence is {Si-Si^{up}}. However, the Si layer just below in the same vertical plane contains vacancies in sample A but not in sample B . The third plane does not contain any vacancies in any layer either for sample A or B and the top layer is still {Si-Si^{up}}. In conclusion, we expect an increase of XPD peak intensities at the corresponding Si^{up} atom angles (Table I) when going from sample A to sample B in Figs. 3(b) and

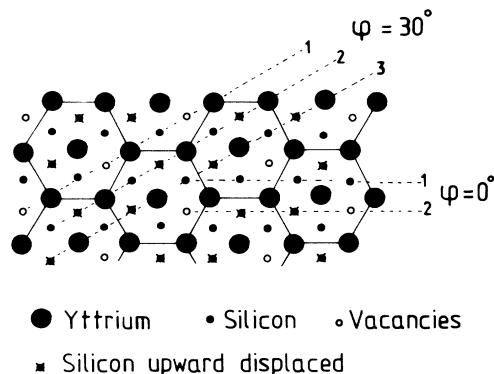


FIG. 2. Crystallographic top-layer structure of the $\text{YSi}_{1.7}$ silicide showing the relative positions of vacancies, unmodified, and upward displaced Si atoms.

3(d). In Fig. 3(b), although the general shape remains the same for samples *A* and *B*, a refined inspection shows that the XPD structures at $\theta=47^\circ$ and especially at 57° increase. The $\theta=57^\circ$ angle enhancement is due to a top-layer Si^{up} atom filling a vacancy while the $\theta=47^\circ$ angle enhancement may be attributed to a Si atom filling a bulk vacancy. Unfortunately, the other relevant angles are too close to bulk Y-Si or Y-Y internuclear angles to be seen. The weakness of the anisotropy prohibits such a comparison in Fig. 3(d).

In summary, we have for the first time determined the surface crystallographies of YSi_{2-x} ($x=0.3$ and $x=0$) using XPD experiments combined with multiple-scattering calculations. Their bulk structure is close to the AlB_2 one. However, the nonstoichiometric $\text{YSi}_{1.7}$ presents an ordered bulk superlattice of vacancies which gives a $\sqrt{3}\times\sqrt{3}$ mesh in the Si surface plane observable by LEED. These vacancies are filled in the stoichiometric YSi_2 case. In both cases, a double XPD structure at $\theta=39^\circ$ and 47° in the Y 3d polar curve at $\phi=30^\circ$ signs the double Si layer surface termination due to a displacement upward (0.8 Å) of one out of two within the top layer. Thus, this surface geometry is similar to a (1×1) Si(111) surface which may serve as a good starting point of a perfect Si(111) overgrowth to produce Si-Y-silicide epitaxial sandwiches.

The authors wish to thank Dr. E. L. Bullock and Dr. D. Sebilliau for their comments on this manuscript.

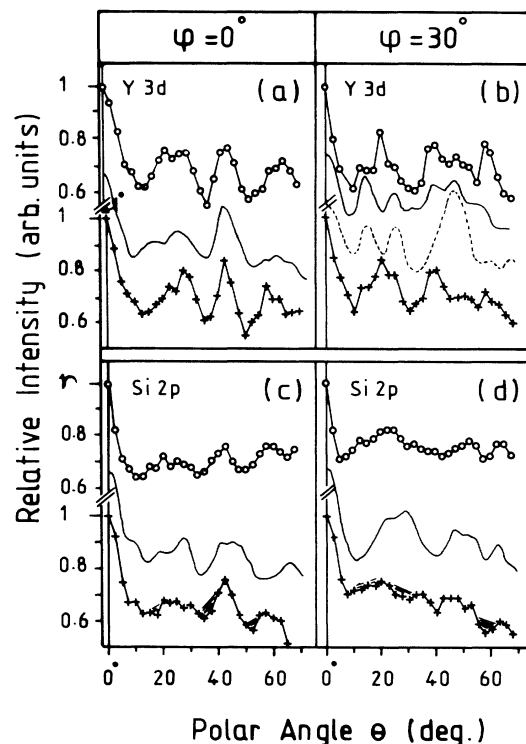


FIG. 3. Experimental polar intensity distribution from samples *A* and *B* yttrium silicides: (+, sample *A*; O, sample *B*) and quasidynamical calculations of yttrium-silicide polar intensities [---, calculation with bulk termination by a flat Si layer; —, calculation with termination by a Si buckled double layer as in Si(111)]. (a) Y 3d at $\phi=0^\circ$; (b) Y 3d at $\phi=30^\circ$; (c) Si 2p at $\phi=0^\circ$; (d) Si 2p at $\phi=30^\circ$.

⁶M. Gurvitch, A. F. J. Levi, R. T. Tung, and S. Nakahara, *Appl. Phys. Lett.* **51**, 311 (1987).

⁷R. Baptist, A. Pellisier, and G. Chauvet, *Solid State Commun.* **68**, 555 (1988).

⁸R. Baptist and E. Hewatt (to be published).

⁹M. Gurvitch, L. Manchanda, and J. M. Gibson, *Appl. Phys. Lett.* **51**, 919 (1987).

¹⁰L. Martinage, *J. Phys. Condens. Matter* **1**, 2593 (1989).

¹¹C. S. Fadley, in *Progress in Surface Science*, edited by S. G. Davison (Pergamon, Oxford, 1984), Vol. 16, p. 275.

¹²W. F. Egelhoff, Jr., *Phys. Rev. B* **30**, 1052 (1984).

¹³H. C. Poon and S. Y. Tong, *Phys. Rev. B* **30**, 6211 (1984).

¹⁴W. F. Egelhoff, Jr., *Phys. Rev. Lett.* **59**, 559 (1987).

¹⁵D. A. Steigerwald, I. Jacob, and W. F. Egelhoff, Jr., *Surf. Sci.* **202**, 472 (1988).

¹⁶W. F. Egelhoff, Jr., D. A. Steigerwald, J. E. Rowe, and T. D. Bussing, *J. Vac. Sci. Technol. A* **6**, 1495 (1988).

¹⁷W. F. Egelhoff, Jr., *J. Vac. Sci. Technol. A* **6**, 730 (1988).

¹⁸G. Grenet, Y. Jugnet, S. Holmberg, H. C. Poon, and Tran Minh Duc, in *Proceedings of the International Conference on Quantitative Surface Analysis*, Teddington, 1988 [*Surf. Interface Anal.* (to be published)].

¹⁹S. Y. Tong, H. C. Poon, and D. R. Snider, *Phys. Rev. B* **32**, 2086 (1985).

²⁰C. H. Li and S. Y. Tong, *Phys. Rev. Lett.* **43**, 526 (1978).

¹R. T. Tung, J. M. Gibson, and J. M. Poate, *Phys. Rev. Lett.* **50**, 429 (1988).

²J. Vrijmoeth, A. G. Schins, and J. F. Van der Veen, *Phys. Rev. B* **40**, 3121 (1989).

³S. A. Chambers, S. B. Anderson, H. W. Chen, and J. H. Weaver, *Phys. Rev. B* **34**, 913 (1986).

⁴J. A. Knapp and S. T. Picraux, *Appl. Phys. Lett.* **48**, 466 (1986).

⁵J. A. Knapp and S. T. Picraux, *Mater. Res. Soc. Symp. Proc.* **54**, 261 (1988).